Icosahedral ordering in supercooled liquids and metallic glasses

Subir Sachdev

Center for Theoretical Physics, P.O. Box 6666
Yale University, New Haven, CT 06511

Published in *Bond Orientational Order in Condensed Matter Systems*, K.J. Strandburg ed.,

Springer-Verlag, New York (1992).

CONTENTS

5.1 Introduction

A metallic glass is a solid consisting of metallic atoms arranged in a random manner with no obvious long-range correlation in the atomic positions. While such random atomic arrangements are easy to achieve in materials with covalent bonding, until 1960 the solid state of all known metals and metallic alloys consisted of regular, periodic arrangements of the atoms. The first metallic glass was produced in 1960 by Duwez and coworkers [1] by rapidly cooling a molten alloy of gold and silicon. Metallic glasses have since then been created in large numbers of simple metal, transition metal and metalloid systems by a variety of ingenious methods. 'Splat-cooling' techniques have been developed to achieve cooling rates of over a million degrees per second and have created a completely new metallurgical technology. The new metallic materials so produced have proved to be of considerable technological importance for their unique magnetic, mechanical and corrosion-resistance properties [2].

In this chapter we investigate the question of how 'random' the atomic arrangements in a metallic glass really are. In particular, an attempt shall be made to identify features of the structure which are not sensitive to the microscopic details like the nature of the interatomic potential, directional bonding and local charge transfer between the atoms. Our analysis shall therefore based upon understanding the structural properties of dense and supercooled systems of atoms interacting with each other through spherically symmetric forces. We find that there are significant short-range orientational correlations between the atomic arrangements: the characterization of these orientational correlations will be the main subject of this paper.

As constructed, the theories reviewed in this chapter are directly applicable to any dense, supercooled liquid of spheres interacting with a pair-potential which has a repulsive hard-core and a weak long-range attraction. Such systems can be easily realized in computer

simulations, but there is no known bulk monoatomic metallic glass. However amorphous films of cobalt and iron have been made by deposition of the metallic vapor on a substrate at liquid helium temperatures. We will compare our results with X-ray scattering measurements on such films. We shall also argue that our results can also be applied to a large class of real metallic glasses: glass forming metal-metalloid and metal-metal alloys.

A key property of the systems we shall consider is that they are frustrated. By 'frustration' we mean that particles in the ground state cannot simultaneously sit in the minima presented to them by pairwise interactions with their neighbors. This leads to a large degeneracy in the ground state. In phase space, the system has large numbers of nearly equal free energy minima separated by substantial free energy barriers. If the system gets locked into one of these minima upon cooling from the liquid, a glassy or amorphous state can result. Our main objective shall be to determine the atomic correlations at a 'typical' local minimum of the free energy.

5.2 Three-dimensional sphere packings and frustration

In this section we shall introduce several qualitative methods of characterizing the order in supercooled liquids. A quantitative approach shall be taken in the next section after the introduction of a suitably defined order-parameter and associated Landau free energy. As noted above, we shall be interested in characterizing the local minima of a system of interacting particles with a Lennard-Jones like pair potential; *i.e.* a potential with a strong hard core repulsion and the a long attractive tail. A related problem we shall also consider is the dense random packing of identical spheres.

The sphere-packing problem has a trivial solution when the spheres are constrained to move in a single plane. Three spheres will clearly lie at the vertices of an equilateral triangle.

Four spheres will form two equilateral triangles sharing a common edge. It is clear that we can extend the arrangement of equilateral triangles to the triangular lattice and accommodate an infinite number of spheres. This packing is the densest possible packing and all particles sit in the minima of the potential due to their six nearest neighbors. Thus the locally optimum arrangement of three spheres (the triangle) has a unique periodic extension and the system is clearly unfrustrated.

The physics changes dramatically when we allow the particles to move in three dimensions. The state of minimum energy for four particles is the tetrahedron, shown in Fig 1. Computer simulations of a Lennard-Jones system [3] show that larger numbers of particles like to arrange themselves in configurations that maximize the number of tetrahedra. In Figs. 2 and 3 we show systems of seven and thirteen particles whose states of global minimum energy are the pentagonal bipyramid and the icosahedron respectively. Both the configurations can be divided very simply into tetrahedra: the pentagonal bipyramid has five tetrahedra around the central bond. The icosahedron is in turn made up of 12 interpenetrating pentagonal bipyramids centered on the 12 bonds from the center to the vertices of the icosahedron. Another important local minimum is the 6 particle octahedral arrangement shown in Fig 4; unlike the previous configurations it cannot be split into approximately equilateral tetrahedra. Note however that the octahedron has an appreciable 'hole' in the middle, indicating that it is a poor starting point in the search for metastable minima for larger numbers of particles.

One manifestation of the frustration in the packing of these particles, is the fact that the bond lengths in the pentagonal bipyramid and the icosahedron are not all equal. The bonds in the center of both solids are approximately 5% smaller than the bonds on the surface. Alternatively, if one attempted to put five perfect tetrahedra around a bond one would be

left with a gap of 7.4 degrees between the first and last tetrahedron. See Fig 5. This situation is in sharp contrast to the case in flat two-dimensional space where six equilateral triangles form a perfect hexagon.

We now turn to the analysis of simulations on the dense-packing of spheres. We shall examine both computer simulations and actual experiments on the dense packing of arrays of ball bearings. An important tool in the analysis of such configurations is the Voronoi construction. The region of space closer to an atom than to any other is identified as the Voronoi polyhedron associated with that atom. Two atoms are then identified as nearest neighbors if their Voronoi polyhedra share a common face. The network of nearest neighbor bonds obtained in this manner can be shown to consist only of tetrahedra (barring exceptional degeneracies). The decomposition of space into a tetrahedral network is physically meaningful only if all the tetrahedra are approximately equilateral and the number of nearly octahedral arrangements relatively small.

One of the early experiments on the packing of ball-bearing arrays was carried out by Bernal [4]. Finney [5] performed a Voronoi decomposition of the Bernal structure and found that 45% of the bonds were the centers of pentagonal bipyramids. Further dense packing experiments were performed by Bennett [6] who used an algorithm designed to give structures denser than those obtained by Bernal. A relaxation by Ichikawa [7] of the Bernal structure and a subsequent Voronoi analysis yielded pentagonal bipyramids on 52% of the bonds. Moreover Finney and Wallace [8] found that the Bennett structure could be well described by local configurations which were either approximately equilateral tetrahedra or octahedra: over 80% of the local configurations were tetrahedra. This latter fact justifies the use of the Voronoi construction in Ichikawa's analysis of the structure.

The theory of metallic glass structure we review here attaches particular importance to

the bonds with five tetrahedra around them ('five-fold' bonds, Fig 2) as a structural motif. The pentagonal bipyramid is the densest possible packing of 7 particles and can thus be regarded as a locally ideal ordered configuration; this notion of ordering will be made precise in the next section. The system would clearly like to extend the five-fold bonds into all space but the geometrical properties of flat three dimensional space make this impossible. Instead, as the dense packing simulations discussed above show, as many as 48% of the bonds turn out to be either six-fold (Fig 6) or four-fold (Fig 7). The four-fold bonds are actually distorted octahedra and the issue of whether they are better regarded as a collection of four tetrahedra or as an octahedron can be decided by examining the bond-lengths: such a criterion was used by Finney and Wallace [8] in the work discussed in the previous paragraph. The Voronoi construction will, of course, always yield only tetrahedra.

Following Nelson [9], we will describe an instantaneous snapshot of a dense supercooled liquid in terms of its arrangement of five-fold bonds. If a particle has twelve five-fold bonds emerging from it, its co-ordination shell will from an icosahedron (Fig 3). Nelson [9] therefore introduced an orientational order parameter which would acquire its maximum value at a particle at the center of an icosahedron. The four-fold and six-fold bonds could then be identified as positive and negative disclination defects in the ideal icosahedral order. The connection with the bond orientational order in two-dimensional hexatics (Chapters 2-4) is apparent: in this case the perfectly ordered sites are particles with six neighbors and the five and seven fold coordinated particles form disclination defects in the orientational order. There is however a crucial difference between these two systems: the defects in two-dimensional hexatics are induced purely by thermal fluctuations; in contrast the four-fold and six-fold bonds are forced into any random close packing of spheres by the frustration inherent in flat three dimensional space. The defects are quite dense: a bond is defected with

probability close to 1/2. Assuming that the defects are randomly distributed, the probability that a particle will have exactly 12 five-fold bonds emerging from it is smaller than 1 in 1000. In their molecular dynamics simulation of 999 particles, Finney and Wallace [8] did not find a single icosahedron: this is not surprising in the light of the above discussion.

We note also the work of Steinhardt *et. al.* [10] which focussed attention on the importance of five-fold bipyramids. In a computer simulation of a super-cooled Lennard-Jones liquid, these investigators examined the system for the presence of bond-orientational order associated with five-fold bonds and icosahedra. They found orientational order at sufficiently low temperatures with a correlation length comparable to the size of the system.

5.2.1 Frank-Kasper phases

Just prior to the work of Bernal and followers, was the analysis of Frank and Kasper [11] of certain inter-metallic crystalline alloys. They noted that a large number of intermetallic compounds (the Laves phases $MgCu_2$, $MgZn_2$, $CaZn_5$, the μ-phase Fe_7W_6, $CaCu_5$, $NbNi$ to name a few; these compounds are now widely referred to as the Frank-Kasper phases) could be understood as representations of tetrahedral close packings. The entire crystal structure was composed of approximately equilateral tetrahedra. A majority of the bonds are five-fold, with the remaining bonds begin six-fold (these phases have no four-fold bonds). Frank and Kasper also presented a simple and important topological argument which showed that no particle could have five-fold bonds and just a *single* six-fold bond emerging from it. In other words, the six fold bonds must form defect lines which run through the entire crystal structure. A particle with a single defect line running through it would then have two six fold bonds emerging from it and have a co-ordination shell of 14 particles (Fig 8a). Frank and Kasper also showed that three or four defect lines could meet at a point; the particle at the intersection of the lines would then have co-ordination shells of 15 or 16 particles

respectively (Fig 8b and 8c). Examples of 12,14,15, and 16 co-ordinated particles occur in the Frank-Kasper phases.

Nelson [9] argued that the defect line analysis of Frank and Kasper could be extended to provide a description of supercooled liquids and metallic glasses. It is a remarkable fact that most of the metallic alloys which from metallic glasses also form stable intermetallic compounds with a Frank-Kasper like structure [12, 13, 14] (this point will be discussed further in Section 5.4.2). However as the computer simulations clearly show, random close-packings also have four-fold bonds which are absent in the Frank-Kasper phases. Using modern topological methods [15], Nelson extended the arguments of Frank and Kasper to include four-fold defect lines. He showed that, like the six-fold bonds, the four-fold bonds could not end at a point and must be part of defect lines. Two, three and four four-fold bonds can meet at a particle, making that particle eight, nine and ten co-ordinated (Fig 9). Super-cooled liquids and metallic glasses therefore form a tangled network of defect lines: an ordered arrangement of defect lines leads to the Frank-Kasper phases.

5.3 Structure factor of monoatomic supercooled liquids

In this section we shall review recent work on constructing a Landau free energy of a dense supercooled liquid of spheres interacting with a pair-potential with a repulsive hard-core and a weak long-range attraction. A gaussian approximation to the Landau free energy will then be used to calculated the experimentally measurable structure factor.

5.3.1 Sphere packings in curved three-dimensional space

A crucial first step in the analysis of any frustrated system is the understanding of the related unfrustrated system which is perfectly ordered. The unfrustrated system can then be used to define an order parameter, which is in turn used to characterize the unfrustrated

system. The ideal, unfrustrated system associated with random close packing of spheres was first identified by Coxeter [16]. He noted that on the three-dimensional surface of a four-dimensional sphere five perfect tetrahedra can be arranged around a bond with no gap left between the first and last tetrahedron *i.e.* the gap in Fig 5 vanishes on this positively curved three-dimensional space. The entire surface of the sphere can be tiled with 600 perfect tetrahedra, with every tetrahedron being equivalent to any other. Every bond has exactly five perfect tetrahedra around it and every particle sits at the center of a perfect icosahedron. This packing of particles of the surface of a surface is known as polytope {3,3,5}. The curvature of the sphere κ, which is the inverse of the radius of the sphere, is related to the near neighbor distance d by

$$\kappa d = \frac{\pi}{5} \tag{1}$$

This tiling of particles can be considered as the analog of the triangular lattice in two dimensions, with the important difference that it is of finite extent.

Motivated by his analysis of polytope {3,3,5}, Coxeter [16] presented a simple 'mean-field' analysis of the effects of frustration in flat space. He argued that some of the properties of dense random packings in flat space could be modeled by a fictitious space-filling polytope $\{3, 3, q\}$, where q is the average number of tetrahedra around a bond. On the surface of a sphere there are five tetrahedra around every bond, so q is 5. In flat space the dihedral angle of the tetrahedron is arcos(1/3), so on the average, there is space for

$$\begin{aligned} q &= \frac{2\pi}{\arccos(1/3)} \\ &\approx 5.1043 \end{aligned} \tag{2}$$

tetrahedra around every bond. The values of q in simulations of supercooled liquids and in the Frank-Kasper phases are quite close to this value [9]. Most remarkable is the Frank-

Kasper phase $Mg_{32}(AlZn)_{49}$, which has a which approaches the ideal value of q to one part in 10^4.

The correlations in polytope {3,3,5} were used as a template for the description of local order in supercooled liquids by Kléman and Sadoc [17], Sadoc [18] and Sadoc and Mosseri [19]. These investigators concentrated upon literal mappings of tetrahedra from curved unfrustrated space to a flat frustrated space.

5.3.2 Order parameter

The particular approach to extending Coxeter's ideas that we shall focus on this chapter was pioneered by Nelson and Widom [20]. An order parameter will be introduced to measure the strength of the local icosahedral ordering. With *each* point in the physical flat three dimensional space associate a tangent four dimensional sphere. Now project the particle density in a small averaging volume ΔV upon the surface of the sphere as shown in Fig 10. This defines a density function $\rho(\vec{r}, \hat{u})$ at every point $\vec{r}$ in three dimensional space and every point $\hat{u}$ on the surface of the tangent sphere at $\vec{r}$. The physical density which is measured by X-ray scattering is clearly $\rho(\vec{r}, \hat{u} = -1)$, where $\hat{u} = -1$ is the 'south pole' of the four-dimensional sphere. The physical question we wish to answer is: how close is the environment in the physical flat three dimensional space around any given point $\vec{R}$ to the ideal ordering in polytope {3,3,5} ? Because of the nature of the projection operation, it is clear that an equivalent question is: how close is the density $\rho(\vec{r} = \vec{R}, \hat{u})$, as a function of $\hat{u}$ near $\hat{u} = -1$, to that of polytope {3,3,5} ? This question is most easily answered by performing an expansion of the density on the sphere in terms of the hyperspherical harmonics [21]:

$$\rho(\vec{r}, \hat{u}) = \sum_{n,m_a,m_b} Q_{n,m_a,m_b}(\vec{r}) Y^*_{n,m_a,m_b}(\hat{u}) \tag{3}$$

where the Y_{n,m_a,m_b} are known hyperspherical harmonics labeled by the representation index $n = 0, 1, 2 \ldots$ and the quantum numbers m_a, m_b, ranging in integer steps from $-n/2$ to $n/2$, label the basis states within each representation of $SO(4)$. The coefficients $Q_{n,m_a,m_b}(\vec{r})$ are defined on every point $\vec{r}$ of the physical space and characterize the environment in the neighborhood of the point $\vec{r}$. They can therefore be considered as a peculiar set of local multi-particle correlation functions. Let $\rho(\vec{r} = \vec{R}, \hat{u})$ specify a density, as a function of $\hat{u}$ on the surface of the sphere, which is identical to the density on polytope {3,3,5}. A simple computation [20] then shows that the order-parameter $Q_{n,m_a,m_b}(\vec{R})$ is zero for all values of n except the special values $n = 12, 20, 24, 30, 32 \ldots$. The precise values of $\vec{Q}_n(\vec{R})$ depend upon location and orientation of polytope {3,3,5} on the sphere, but the selection rules on n are independent of these parameters. The vanishing of $\vec{Q}_n(\vec{R})$ on such a large number of n values is a consequence of the high degree of symmetry of polytope {3,3,5}. The special set of n values $12, 20, 24, 30, 32 \ldots$ thus form *a 'reciprocal lattice'* distinguishing polytope {3,3,5} from other particle arrangement on the surface of the sphere. We are now finally in a position to answer the questions posed earlier in this paragraph. The particle configuration in the neighborhood of $\vec{R}$ is similar to that in polytope {3,3,5} if the values of $\vec{Q}_n(\vec{R})$ are largest at the following special values of $n = 12, 20, 24, 30, 32 \ldots$. The matrices $\vec{Q}_n(\vec{r})$ for these special values of n are therefore the order parameters that we require. These order parameters characterize the degree of tetrahedral and five-fold bipyramidal ordering in the neighborhood of any point in space.

Before we are able to write down a Landau free energy with the order parameter introduced above, we need to understand the optimum relative position of two fragments of polytope {3,3,5} at neighboring point in space. A simple way achieving the best relative positions which minimize the number of defect lines was suggested by Sethna [22]. Imagine

"rolling" the four-dimensional sphere along a straight line in flat three-dimensional space. The particle configuration laid out by this procedure will consist of mildly distorted tetrahedra and not induce any defect lines. In fact the tetrahedra will form a Bernal spiral shown in Fig 11. (Precisely such spirals exist along the axes of the Kagomé net structure found in many Frank Kasper phases.) The relative orientation of the order parameter at two neighboring points along the rolling line can be easily shown to satisfy

$$\vec{Q}_n(\vec{r}+\vec{\delta}) = \exp\left(i\kappa \mathbf{L}^n_{0\mu}\delta_\mu\right)\vec{Q}_n(\vec{r}) \tag{4}$$

where $\mathbf{L}^n_{0\mu}$ is a $(n+1)\times(n+1)$ matrix which generates the rotations of $SO(4)$ performed when the sphere is rolled in the μ direction of flat three dimensional space. One might now naively guess that it should be possible to tile all of three-dimensional space with fragments of polytope {3,3,5} by starting at origin and rolling the sphere in a straight line in all directions. However it can be shown that this procedure always introduces incompatibilities at points other than the origin. One way to illustrate this frustration is to consider the operation of rolling the sphere in a closed path along the edges of a square in the μ and ν directions as shown in Fig 12 5.12. The order parameter configuration before and after the rolling operations will have the following relationship [22]

$$\begin{aligned}
\vec{Q}_n(\vec{r})|_{\text{final}} &= \exp\left(-i\kappa\mathbf{L}^n_{0\mu}a\right)\exp\left(-i\kappa\mathbf{L}^n_{0\nu}a\right)\exp\left(i\kappa\mathbf{L}^n_{0\mu}a\right)\exp\left(i\kappa\mathbf{L}^n_{0\nu}a\right)\vec{Q}_n(\vec{r})|_{\text{initial}} \\
&\approx \exp\left(-\kappa[\mathbf{L}^n_{0\mu},\mathbf{L}^n_{0\nu}]a^2\right)\vec{Q}_n(\vec{r})|_{\text{initial}} \\
&= \exp\left(-i\kappa\mathbf{L}^n_{\mu\nu},a^2\right)\vec{Q}_n(\vec{r})|_{\text{initial}}
\end{aligned} \tag{5}$$

where $\mathbf{L}^n_{\mu\nu}$ is the generator of $SO(4)$ which performs rotations in the (μ,ν) plane of flat three-dimensional space. The relative rotations between the initial and final configurations of the order parameter necessarily imply the presence of a constant density of disclination defect lines piercing every plaquette in flat three dimensional space. These are precisely the

four-fold and six-fold bonds introduced earlier; the sign of the rotation above implies an excess of six-fold bonds over four-fold bonds.

5.3.3 Landau free energy

We now finally have assembled all the ingredients necessary in writing down a Landau theory of tetrahedral close packing in supercooled liquids. The Landau free energy expansion performs an expansion in gradients and powers of the order parameter retaining all terms which are consistent with the symmetry of the system. Because of the strong frustration inherent in flat three dimensional space we anticipate that the magnitude of $\vec{Q}$ will be small and that a low-order expansion will be adequate. To quadratic order the free energy takes the form [20]

$$F = \frac{1}{2}\sum_n \int d^3\vec{r}\left[K_n \left|\left(\partial_\mu - i\kappa \mathbf{L}^n_{0\mu}\right)\vec{Q}_n\right|^2 + r_n\left|\vec{Q}_n\right|^2\right] + \cdots \tag{6}$$

where the ellipses denote cubic and higher order terms, and K_n and r_n phenomenological parameters. The gradient term has been chosen such that the system will attempt to satisfy the 'rolling-sphere' relationship (Eqn 4) at every point in space. Apart from this input, the form of the free energy follows solely from the symmetry requirement that the energy be independent of the orientation of polytope {3,3,5} defined by the order-parameter $\vec{Q}_n$. We make the physical input of demanding local regions of polytope {3,3,5} ordering by demanding that the $r_n \to +\infty$ except for the selected values $n = 12, 20, 24, 30, 32\ldots$ [23]. Fluctuations in all but these values of n will be strongly suppressed.

Before turning to an analysis of the free energy F, it is useful at this point to recall a few essential features of a related system - an extreme type-II superconductor in a magnetic field [24] (by extreme type-II we mean that the London penetration depth is so large that we can safely ignore the changes in the external magnetic field due to the supercurrents). In

suitable units, the Landau free energy expansion of the superconducting order parameter Ψ takes the form:

$$F_{sc} = \frac{1}{2} \int d^3\vec{r} \left[K \left| (\partial_\mu - iA_\mu) \Psi \right|^2 + r \left| \Psi \right|^2 \right] + \cdots \tag{7}$$

where $\vec{A}(\vec{r})$ is the vector potential associated with a uniform external magnetic field $\vec{H}$ ($\vec{\nabla} \times \vec{A} = \vec{H}$), K is a phenomenological stiffness, and the parameter r is assumed to have the form $r = r'(T - T_c)$. The mean-field phase diagram for this system as a function of the temperature T and H is sketched in Fig 13b. In zero field the system goes superconducting when $r = 0$, *i.e.* at $T = T_c$. In non-zero fields the *frustration* induced by the external field has two consequences: (i) it depresses the transition temperature: i.e. the system does not go superconducting until r is sufficiently negative; and (ii) the superconducting state in non-zero field is an Abrikosov flux lattice consisting of a regular array of defect lines (vortices) at a density which relieves the frustration due to the field.

We now return to the consideration of the physics of icosahedral ordering as described the free energy F. As discussed earlier, we can turn off the frustration by placing the particles on the surface of a four-dimensional sphere of radius R [25]. When the curvature of the sphere $\kappa = 1/R$ satisfies the condition (1), the system is unfrustrated and we can replace the 'covariant' derivative in Eqn (6) by an ordinary derivative. This unfrustrated system is the analog of the superconductor in zero field, with the low-temperature ordered state being polytope {3,3,5}. The parameters r_n are presumably close to zero at melting temperature of polytope {3,3,5}: they are not exactly zero because the presence of cubic terms in the free energy expansion drive the transition first order. As R moves away from the ordered value, the melting temperature is depressed and the ordered state becomes a Frank-Kasper structure consisting of an ordered configuration of defect lines: the phase diagram is shown in Fig 13a. The Frank-Kasper structures are the analog of the Abrokosov

flux lattice in the superconductor. The physical flat three dimensional space is strongly frustrated, and we presume that sluggish dynamics freezes the system at a temperature T_g which is above the temperature T_0^*, the melting temperature of a suitable Frank-Kasper structure. We also denote in Fig 13a the melting temperature T_m of the global ground state of a monoatomic metallic system which is usually a FCC crystal. An important prediction that can be made from the above considerations is that the parameters r_n must be *negative* for $n = 12, 20, 24, 30, 32 \ldots$ at the glass transition temperature.

We turn finally to the use of the free energy F to make quantitative experimental predictions [23, 24]. We will calculate the structure factor $S(\vec{q})$,

$$S(\vec{q}) = \int d^3\vec{R} e^{i\vec{q}.\vec{R}} \left\langle \rho(\vec{r} = \vec{R}, \hat{u} = -1)\rho(\vec{r} = 0, \hat{u} = -1) \right\rangle , \tag{8}$$

which can be measured easily in electron, X-ray, or neutron scattering experiments. We will assume that the glassy configuration frozen in as the liquid is quenched can be adequately described by the equilibrium ensemble defined by F with all cubic and higher order terms omitted. With this working hypothesis, the structure factor can be easily calculated after using the relationship (3) between the order parameter and the density. The first step is the diagonalization of the quadratic form in F; details of this have been presented in Ref. [24]. The diagonalization yields a spectrum of eigenvalues which depend upon the wave-vector q and the representation index n. For physically reasonable values of K_n and r_n, it is easy to see [23, 24] that there is a peak in the structure factor for each of the n values 12,20,24,30,32 and that this peak occurs very close to the wavevector q at which the lowest eigenvalue in the representation n has a minimum as a function of q. Furthermore the relative positions of the peaks are *independent* of all parameters in F. In particular the strongest peaks occur

at the wavevectors q_{12}, q_{20} and q_{24} and these wavevectors are predicted to have the ratios:

$$\frac{q_{20}}{q_{12}} = 1.71 \quad ; \quad \frac{q_{24}}{q_{12}} = 2.04 \tag{9}$$

We show in Table 5.1 a comparison of these ratios to the ratios between the first, second and third peaks in the structure factor of vapor-deposited cobalt and iron, and computer simulations of supercooled liquids: the agreement is remarkably good for q_{20}/q_{12} but there are $\approx 2.5\%$ errors in q_{24}/q_{12}. It is argued in Ref. [24] that the effect of higher terms in the free energy must be of a form which improves the agreement in q_{24}/q_{12}.

Absolute predictions of the peak positions can be made once the parameter κ is known. Using Eqn (1) this involves knowledge of the hard-sphere diameter d. Using experimentally known peak positions we obtain a value of d which is within 10% of the interparticle spacing of crystalline ground states of the relevant atoms. Finally, we can perform a fit to the entire structure factor by using κ, K_n and r_n as adjustable parameters. The results of such a procedure for amorphous cobalt is shown in Fig 14. We find a fourth peak in the structure factor which appears to be a composite of q_{30} and q_{32}. The values of r_n can be determined from the fit, and as expected from the analysis associated with Fig 13, all of them are negative. We have thus obtained a consistent, phenomenological description of metallic glasses and supercooled liquids which associates peaks in the structure factor with symmetry properties of polytope {3,3,5}.

5.4 Application to real metallic glasses

Strictly speaking the calculation outlined above should be applicable only to monoatomic dense supercooled liquids. All of the metallic glasses manufactured so far have two or more metallic or metalloid components of differing sizes. Nevertheless the results obtained above should be of relevance to real metallic glasses for reasons we shall now discuss. All metallic

glasses can be broadly classified into two categories [14]: (i) the metal-metalloid glasses consisting of $M_{1-x}N_x$ where x is in the range 0.15 - 0.20, M is one or more of transition metals like Fe, Co, Ni, Pd, Au, and Pt, and N is one or more of metalloids like P, B, Si, and C; (ii) the metal-metal glasses which contain combinations of metals like Mg, Zn, Ca, Al, Cu, Ti, La and Ce.

5.4.1 Metal-metalloid glasses

We begin with a discussion of the structure and formation of the metal-metalloid glasses. Before turning to specific materials we present some qualitative general arguments. In the spirit of the Landau theory introduced above we can model the effect of the metalloid component by a fluctuating impurity concentration field $c(\vec{r})$. The simplest way that $c(\vec{r})$ can couple to the icosahedral order parameter is via the replacement [23]

$$F \rightarrow F + \int d^3\vec{r} \left(\sum_n \gamma_n |\vec{Q}_n|^2 + \frac{c^2}{2\chi} - c\Delta \right) \tag{10}$$

where χ is the impurity concentration susceptibility, the γ_n are coupling constants, and Δ is an impurity chemical potential. The constants Δ and γ_n must be positive for the impurities to disrupt the local icosahedral ordering. We can now integrate out the impurity concentration and find that the only effect of the field $c(\vec{r})$ is to perform the replacement

$$r_n \rightarrow r_n + \frac{\gamma_n \Delta \chi}{2} \tag{11}$$

From the analysis above it is clear that this replacement merely leads to a broadening of the peaks in the structure factor without significantly changing their positions. This is what is observed experimentally.

As a typical example of a metal-metalloid glass, we shall consider in detail the $Ni-P$ system. Shown in Fig 15 is the equilibrium phase diagram of the $Ni-P$ system. Also marked

is the range of compositions at which the system forms a metallic glass. Note that this range is centered around the deepest eutectic. This is a universal feature among metal-metalloid glasses.

The stable crystal structure near the glass formability range is Ni_3P. A first step in understanding the structure of the metallic glass is an analysis of the structure of Ni_3P [29]. The space group of the crystal is S_4^2, with each unit cell containing 24 Ni atoms in symmetry partners of three non-equivalent positions and 8 P atoms in symmetry partners of one position. We assign nearest neighbor bonds to all $Ni-Ni$ distances which are smaller than 3.58 A and to all $Ni-P$ distances which are less than 2.58 A. These distances are chosen so that the results are equivalent to a 'weighted' [30, 31] Voronoi construction. In Fig 16 we show the co-ordination shell of P. There are 9 Ni nearest neighbors arranged so that all but three of the bonds are fiver-fold. These three bonds are four-fold and the entire structure forms a $Z9$ defect in the notation of Nelson [9]. The P atom in Ni_2P has a very similar co-ordination shell. It is the small size of the P atom which forces in a small co-ordination number and four-fold co-ordinated bonds. The partially covalent nature of the $Ni-P$ bond is also responsible for this structure. The four-fold bonds lead to the presence of distorted octahedra. However, the shortest diagonal of the octahedron is almost 40% smaller than the other two, demonstrating that the octahedra are better described as four-fold bipyramids. The three different co-ordination shells of the Ni atoms are more complicated. They are shown in Fig 17. The majority of the bonds emanating from the Ni are five-fold, with the remaining bonds being either six-fold or four-fold. All the four-fold bipyramids associated with these Ni atoms have at least one P atom on their vertices. The diagonals of the four-fold bipyramids now differ by only 12% so they are more nearly octahedral. However, as discussed below, these octahedra occupy only a small fraction of the space in the unit cell.

In Table 5.2 we display the co-ordination statistics of the Ni and P atoms. In Table 5.3 are displayed the relative fractions of four-fold, five-fold and six-fold bonds in crystalline Ni_3P. For comparison, we have also displayed the relative fractions of these bonds in the relaxed Bennett model of Ichikawa [7]. Note the remarkable similarity between the co-ordination topology of a dense random packing model of *identical* spheres and that of a packing of two different sized spheres. In the case of Ni_3P, it is the smaller size of the P atom which forces in an appreciable number of four-fold bonds. The four-fold bonds in the Ichikawa-Bennett model [7] represent a presence of octahedral 'voids' which will probably decrease in number upon further relaxation.

Experiments of Cocco *et. al.* [32] measuring the radial distribution function of glassy $Pd_{1-x}B_x$ (which we expect to be structurally very similar to $Ni_{1-x}P_x$) showed a small peak at $\sqrt{2}$ times the Pd diameter, indicating the presence of four-fold bipyramids. However the size of the peak *decreased* with decreasing B concentration [32], indicating that the small size of the B atom was responsible for the four-fold bipyramids. Recognizing the importance of the special co-ordination topology of the P atoms, Gaskell [33] has performed a simulation of the structure of *glassy* $Ni_{1-x}P_x$. The model consists essentially of a random packing of phosphorus units having a local environment similar to that of P in Ni_3P shown in Fig 16. Gellatly and Finney [30] performed a Voronoi analysis of this structure using a technique which recognized the size differences between the atoms. The results of this analysis are shown in Table 5.3. Again almost 50% of the bonds are five-fold co-ordinated. There is a larger number of four-fold bonds than in the relaxed Ichikawa-Bennett model, but this is probably because the constructions constrains every phosphorus environment to be that of Fig 16. The main conclusion we wish to draw from all of the above arguments is that the dense random tetrahedral close-packing of spheres remains a good approximation for the

structure of glassy $Ni_{1-x}P_x$. With the additional broadening of the peak widths the analysis based upon polytope {3,3,5} remains valid.

As noted earlier most metal-metalloid glasses form at compositions near the eutectic [2]. This can be most simply understood by the fact that there is no *stable crystalline structure* at the eutectic composition. Increasing the nickel content in the Ni_3P structure will increase the energy of the crystal drastically because the Ni atoms do not prefer to sit at the smaller P sites. There may well be exotic metastable crystal structures with larger unit cells at the eutectic compositions which will accommodate the tendency of the Ni atoms to sit in the center of icosahedra, and, at the same time, enable the P atoms to maintain their environment. However, the four-fold defect lines which are forced in by the P atoms act as kinetic hinderances and lock the system in a metastable glassy state. At even lower P compositions, the pure crystalline Ni structure is stable enough to prevent glass formation. THe importance of the high energies of the crystal structure at the eutectic composition was illustrated by some experiments of Chen [34, 35]. None of the thermodynamic measurements of Chen indicated any extra structural stability of the glassy structure at the eutectic composition.

5.4.2 Metal-metal glasses

Glasses are formed upon the rapid cooling of many molten metal-metal alloys. These glasses may be further classified as (i) simple metal - simple metal glasses such as $Mg_{70}Zn_{30}$, $Ca_{67}Al_{33}$, (ii) simple metal - transition metal glasses such as $Ca_{65}Pd_{35}$, $Ti_{60}Be_{40}$ and (iii) transition metal - transition metal glasses such as $Nb_{60}Ni_{40}$, and $Fe_{55}W_{45}$. Some rare earth alloys also form metallic glasses. A universal feature of these alloys in that at these or at differing compositions they form stable intermetallic compounds which are either Frank-Kasper or closely related structures. For the alloys mentioned above, the associated Frank-Kasper phases are $MgZn_2$, $CaAl_2$, $CaPd_2$, Ti_2Be_{17}, $TiBe_2$, $NbNi$ and Fe_7W_6. As we have al-

ready discussed, all of these crystalline phases are characterized by a tetrahedral network of near neighbor bonds, with all the tetrahedra being approximately equilateral. This supports the conjecture that the disordered glassy arrangements of these alloys are described by tetrahedral close packing. A majority of the bonds will have five tetrahedra around them, interspersed with a tangled network of lines of six-fold and some four-fold bonds.

In these systems, there are compositions at which the Frank-Kasper phases are very stable and prevent effective glass formation. The Laves phase, for instance, will form when one third of the atoms are larger than the rest, the ratio of the radii being in the range 1.1 - 1.3. It is easy to see how requirements of geometrical close-packing of spheres in the Laves phase forces in this requirement. It is important to note, as pointed out by Hafner [14], that changes in the atomic diameter in the presence of the other element of the alloy need to be taken into account. These changes in diameter are controlled by electronegativity differences between the components: the more electropositive atom shrinks in size. At compositions in which the larger atom is in the majority, no stable crystalline structure will form, and the ease of glass formability will increase. In this regard, a calculation performed by Hafner [14] upon the $Ca - Mg$ system is of particular interest. Using a self-consistent pseudopotential method, Hafner estimated the total energies of $Ca - Mg$ Laves phase and the metallic glass as modeled by a relaxed Finney structure. Remarkably, the energy of the glassy structure was a minimum at the *same* composition as the $CaMg_2$ Laves phase. This nonetheless did not include the range of glass formation. At other compositions near the eutectic, the energy of the crystalline structure was driven up considerably, leading to easier glass formation.

5.5 Conclusions

This chapter has reviewed a statistical theory of the packing of identical hard spheres in flat three dimensional space. The theory begins by identifying the tetrahedral arrangement of four spheres as an important locally dense arrangement and proceeds to tile all space with the tetrahedra. Such a task is well known to be impossible for equilateral tetrahedra and distortions are inevitably introduced. Five tetrahedra can pack around a bond with a minimum of distortion (Figure 2). An attempt to continue this five-fold structure to all of space runs up against further geometric obstacles and one finds that six-fold (Fig 6) and four-fold (Fig 7) must be introduced. An orientational/translational order parameter was then introduced to measure the amplitude and the orientation of the five-fold bipyramids (Fig 2). This rather complicated multi-particle order parameter was defined by comparing the local environment in the neighborhood of any point with that of an ideal packing of spheres (polytope $\{3, 3, 5\}$) on a uniformly curved three dimensional space. In this latter packing the curvature of the space has been carefully chosen to allow for a tiling with identical equilateral tetrahedra, thus relieving the frustration of flat three dimensional space. We emphasize that this curved space is used only as a mathematical tool to generate the bond orientational order parameter which describes sphere packings in the physical flat three dimensional space. A Landau free energy was introduced to describe fluctuations of this order parameter in a manner which incorporated the frustration inherent in flat space. The frustration induced disclinations in the order parameter which were identified with the four-fold and six-fold bipyramids. Finally the Landau free energy was used to calculate the structure factor of the hard sphere packing. Parameter free predictions were made for the ratio of the peak positions of the structure factor which were in rather good agreement with experimental measurements on amorphous metallic films. To our knowledge this is the first

theory to present a direct calculation and physical interpretation of the peaks in the structure factor. All existing computer simulations have focussed mainly on the peaks in the radial distribution function, which is a Fourier transform of the structure factor.

The second part of this chapter dealt with the application of these results to realistic metallic glasses which always contain combinations of metallic/metalloid atoms of different sizes. It was argued that peak position in the structure factor of these glasses should be insensitive to the presence of atoms of slightly differing radii: the main effect of the alloying should be a broadening of the peaks, an effect which is borne out experimentally. Monoatomic metallic glasses do not form because of the presence of low crystalline structures with cubic symmetry which pre-empt glass formation. With the introduction of atoms of different sizes these crystalline structures are destabilized and the system is able to access a glassy state. The main shortcoming of our approach is the lack of a precise criterion for the conditions which enhance glass formability. This question has however been addressed with first-principles electronic structure calculations by Hafner [14]

The ideas discussed in this chapter can be applied to other properties of metallic glasses: these include electronic structure [36], phonon density of states [37] and viscous relaxation [38]. The reader is referred to the original papers for details. In the following chapter Jaric will discuss a different, but closely related, formulation of the bond orientational order parameter and its coupling to translation symmetries and quasicrystalline order.

Acknowledgements

All of my work on the subject reviewed in this paper was performed in collaboration with D.R. Nelson; I am grateful to him for freely offering his insights and many useful discussions. This review has been adapted from Chapter 1 of S. Sachdev, Ph. D. Thesis, Harvard University, 1985. The work was supported in part by the National Science Foundation under Grants

No. DMR82-07431 and DMR8857228, and by the Alfred P. Sloan Foundation.

References

[1] W. Klement, R.H. Willens, and P. Duwez, Nature **187**, 809 (1960); for a historical account see P. Duwez, Trans. Am. Soc. Metals **60**, 607 (1967)

[2] For a review see *Amorphous Metallic Alloys* edited by F.E. Luborsky, Butterworth (1983).

[3] M.R. Hoare, Adv. Chem. Phys.. **40**, 49 (1979).

[4] J.D. Bernal, Proc. Roy. Soc. London Ser. A **280**, 299 (1964).

[5] J.L. Finney, Proc. Roy. Soc. London Ser. A **319**, 479 (1979).

[6] C.H. Bennett, J. Appl. Phys. **43**, 2727 (1972).

[7] T. Ichikawa, Phys. Status Solidi **19**, 707 (1973) and T. Yamamoto, H. Shituba, T. Mihara, K. Haga and M. Doyama in *Porc. Int. Conf. on Rapidly Quenched Metals* Vol 1 edited by T. Masumoto and K. Suzuki, Japan Inst. of Metals, Sendai (1982).

[8] J.L. Finney and J. Wallace, J. Non. Cryst. Solids **43**, 165 (1981).

[9] D.R. Nelson, Phys. Rev. B **28**, 5515 (1983).

[10] P.J. Steinhardt, D.R. Nelson, M. Ronchetti, Phys. Rev. Lett. **47**, 1297 (1981); Phys. Rev. B **28**, 784 (1983).

[11] F.C. Frank and J.S. Kasper, Acta Crystrallogr. **11**, 184 (1958) and **12**, 483 (1959)

[12] D.E. Polk and B.C. Giessen, *Metallic Glasses*, Am. Soc. of Metals, Metals Park, Ohio (1978).

[13] R. St. Amand and B.C. Giessen, Scr. Metall. **12**, 1021 (1978)

[14] J. Hafner, Phys. Rev. B **21**, 406 (1980).

[15] N.D. Mermin, Rev. Mod. Phys. **51**, 591 (1979).

[16] H.S.M. Coxeter, Ill. J. Math., **2**, 746 (1958); *Introduction to Geometry*, Wiley (1969); *Regular Polytopes*, Dover, New York (1973).

[17] M. Kléman and J.F. Sadoc, J. Phys. (Paris) Lett. **40**, L569 (1979).

[18] J.F. Sadoc, J. Phys. (Paris) Colloq **41**, C8-326 (1980).

[19] J.F. Sadoc and R. Mosseri, Phil. Mag. B **45**, 467 (1982).

[20] D.R. Nelson and M. Widom, Nucl. Phys. **B240** [FS12], 113 (1984).

[21] M. Bander and C. Itzykson, Rev. Mod. Phys. **38**, 330 (1966).

[22] J.P. Sethna, Phys. Rev. Lett. **50**, 2198 (1983).

[23] S. Sachdev and D.R. Nelson, Phys. Rev. Lett. **53**, 1947 (1984).

[24] S. Sachdev and D.R. Nelson, Phys. Rev. **B32**, 1480 (1985).

[25] J.P. Straley, Phys. Rev. **B30**, 6592 (1984).

[26] P.K. Leung and J.C. Wright, Phil. Mag. **30**, 185 (1974).

[27] J.-P. Lauriat, J. Non-cryst. Solids, **55**, 77 (1983).

[28] J.D. Weeks, Phil. Mag. **35**, 1345 (1977).

[29] B. Aronsson, Acta Chem. Scand. **9**, 137 (1955).

[30] B.J. Gellatly and J.L. Finney, J. Non. Cryst. Solids **50**, 313 (1982).

[31] F.M. Richards, J. Mol. Biol. **82**, 1 (1974).

[32] G. Cocco, S. Enzo, M. Sampoli and L. Schiffni, J. Non. Cryst. Solids **61& 62**, 577 (1984).

[33] P.H. Gaskell, J. Non. Cryst. Solids bf 32, 207 (1979).

[34] H.S. Chen, Acta Metall. **24**, 153 (1976).

[35] H.S. Chen, Mat. Sci. and Engg. **23**, 151 (1976).

[36] M. Widom, Phy. Rev. B **31**, 6456 (1985).

[37] M. Widom, Phy. Rev. B **34**, 756 (1986).

[38] S. Sachdev, Phys. Rev. B **33**, 6395 (1986).

	Theory	Amorphous cobalt [26]	Amorphous Iron [27]	Simulations [28]
q_{20}/q_{12}	1.71	1.69	1.72	1.7
q_{24}/q_{12}	2.04	1.97	1.99	2.0

Table 5.1.

Comparison of the theoretical predictions from the free energy F for the ratio in the peak-positions of the structure factor with experimental measurements on vapor-deposited iron and cobalt and computer simulations on monoatomic supercooled liquids.

Atom	v_4	v_5	v_6	Z
P	3	6	0	9
NiI	1	10	4	15
$NiII$	3	6	7	16
NiI	3	6	5	14

Table 5.2.

Co-ordination statistics for the P and Ni atoms in Ni_3P. The number of n-fold bonds emanating from an atom is represented by v_n. The total co-ordination number of the atom is Z.

Structure	f_4	f_5	f_6	q
Ni_3P	18	52	30	5.12
Ichikawa-Bennett	16	53	27	4.91
Gaskell	27	49	18	4.61

Table 5.3.

Distribution of four-fold, five-fold and six-fold bonds in various structures. The percentage of n-fold bonds is represented by f_n and q is mean number of tetrahedra around a bond.

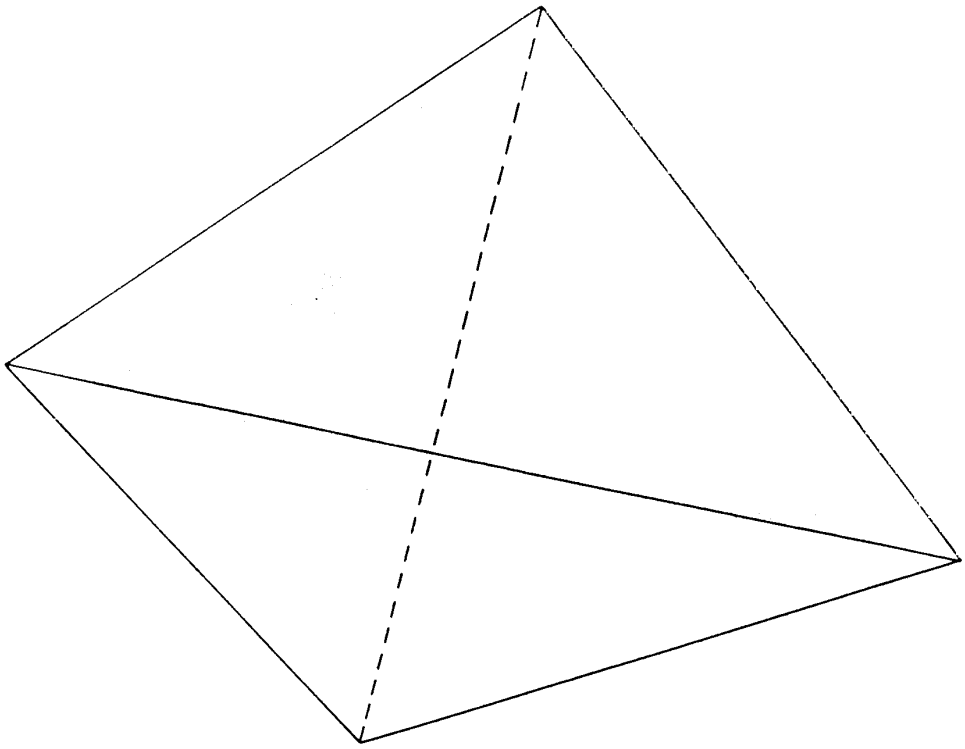

Figure 1: *State of minimum energy for four particles : the tetrahedron.*

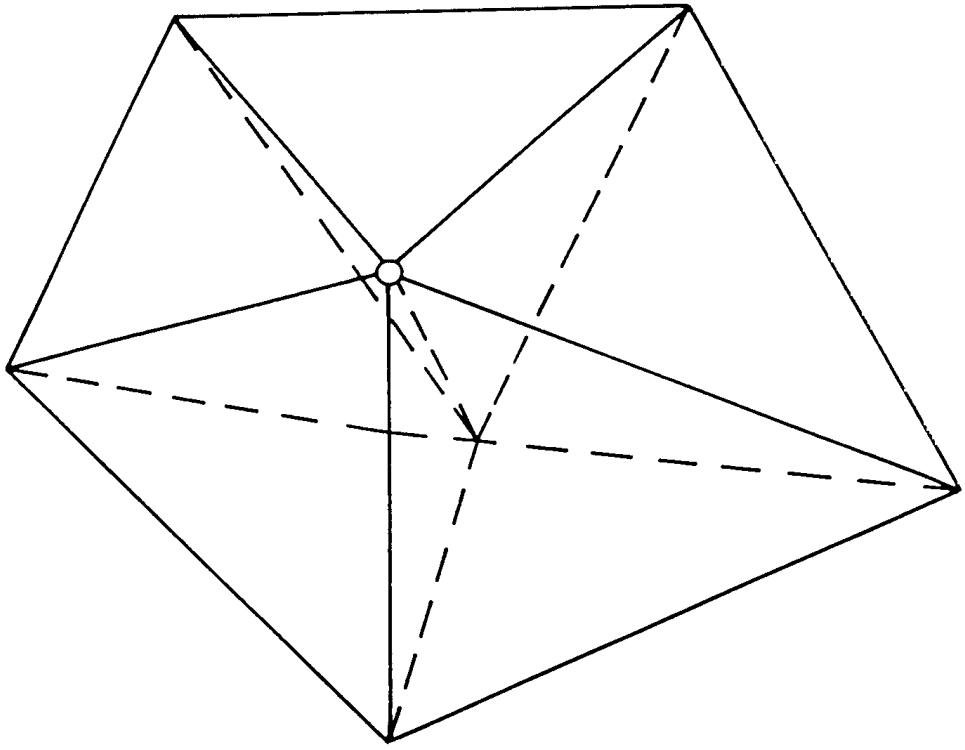

Figure 2: *State of minimum energy for seven particles : five-fold bipyramid.*

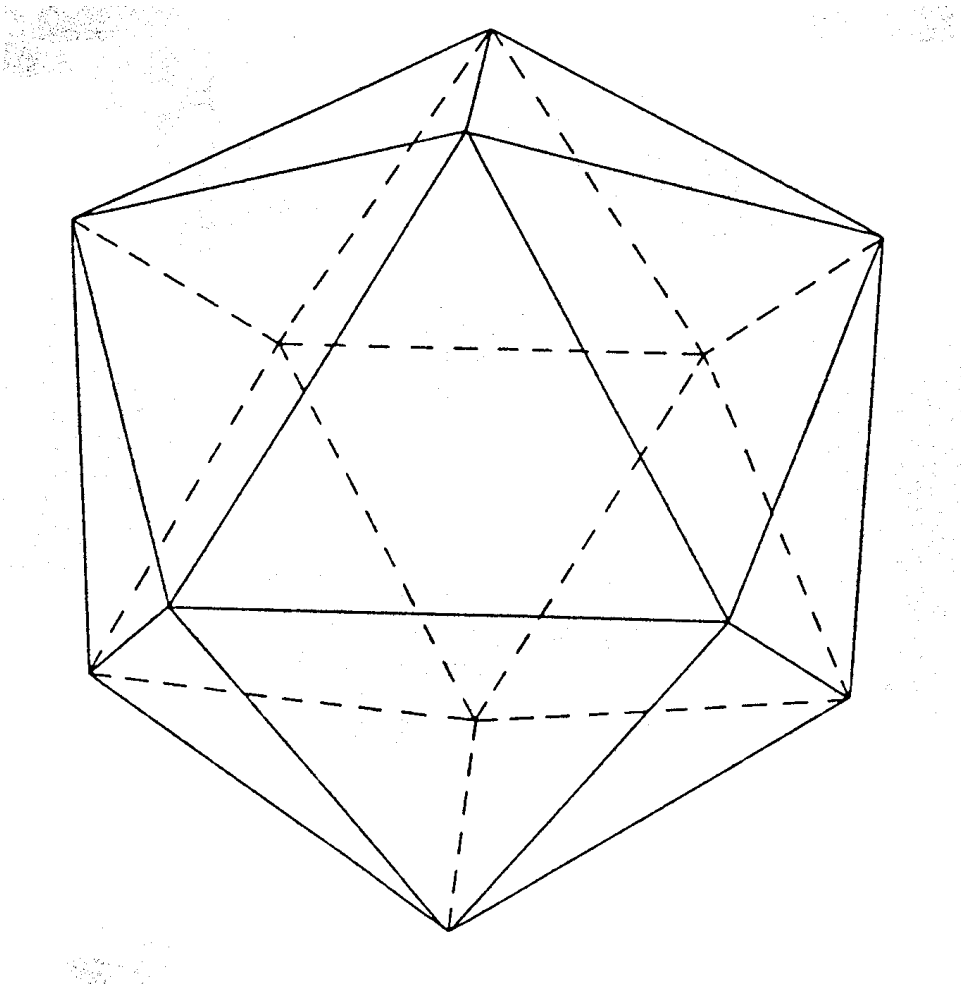

Figure 3: *State of minimum energy for thirteen particles : the icosahedron.*

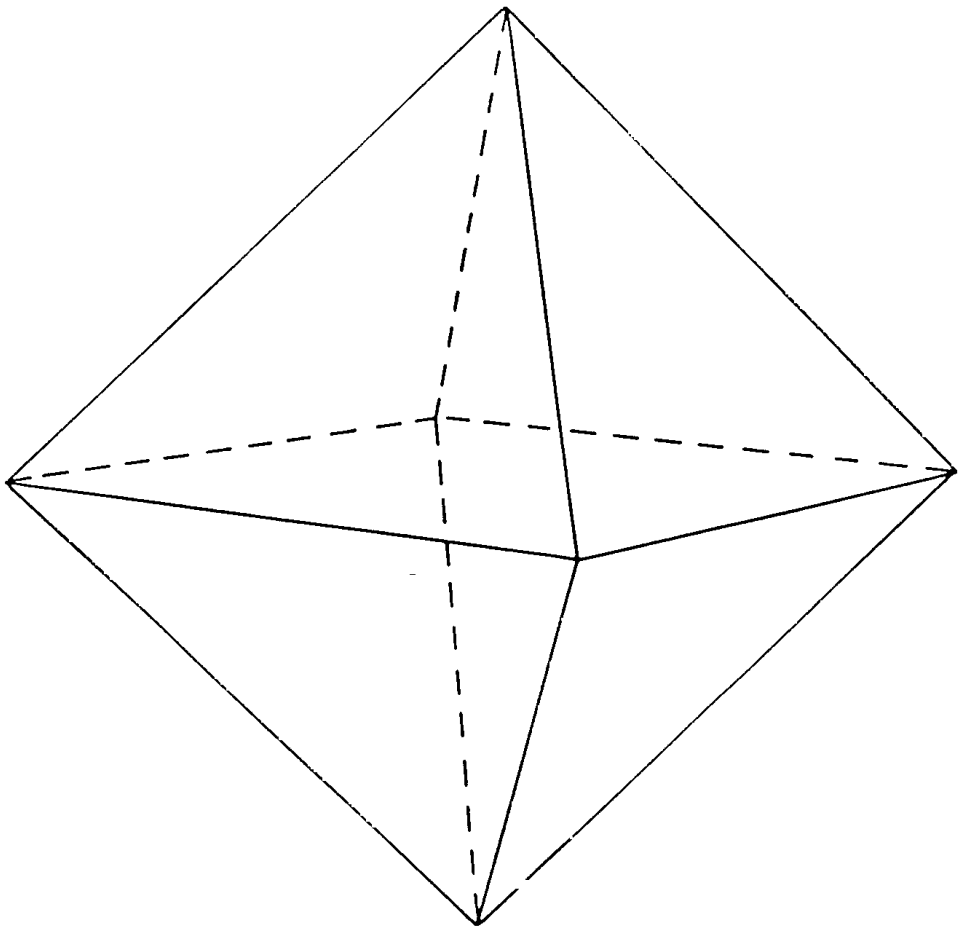

Figure 4: *Local minimum of energy for six particles : the octahedron.*

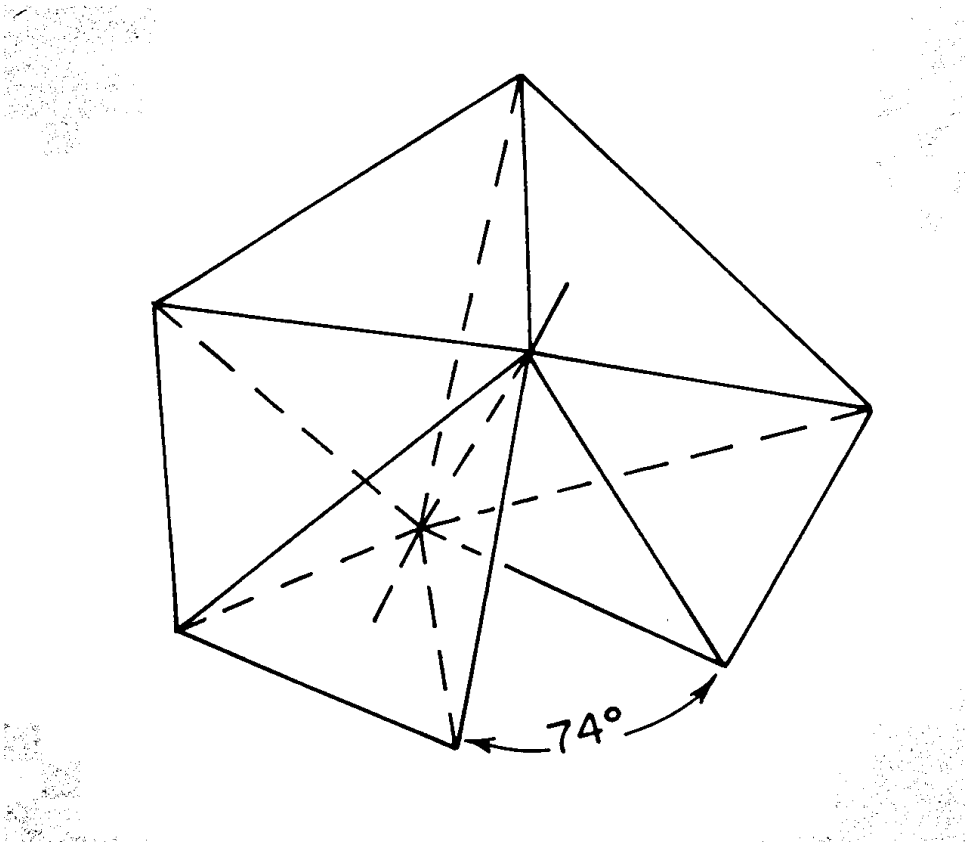

Figure 5: *Five perfect tetrahedra around a bond. Note the empty space of 7.4 degrees which is left over.*

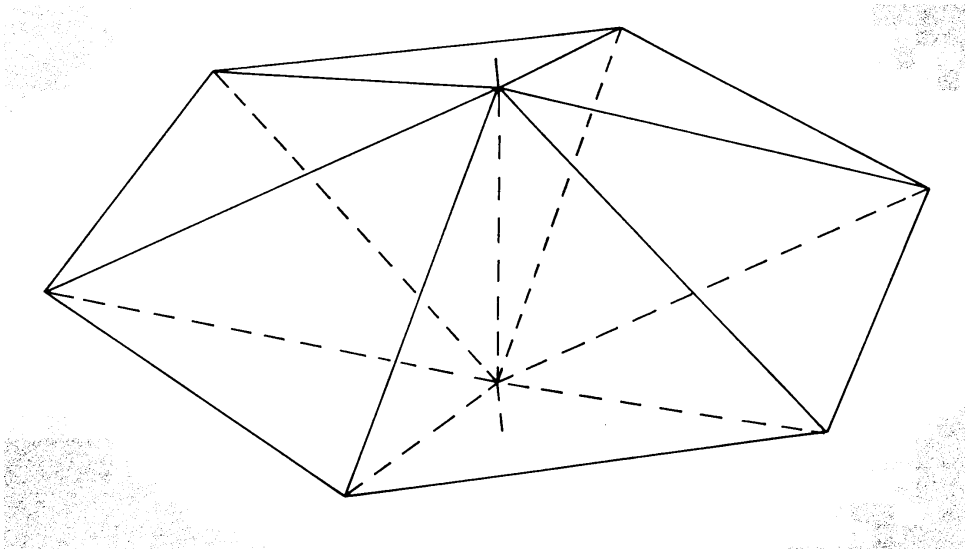

Figure 6: *A six-fold bipyramid. The bond in the center is identified as a -72 degree disclination.*

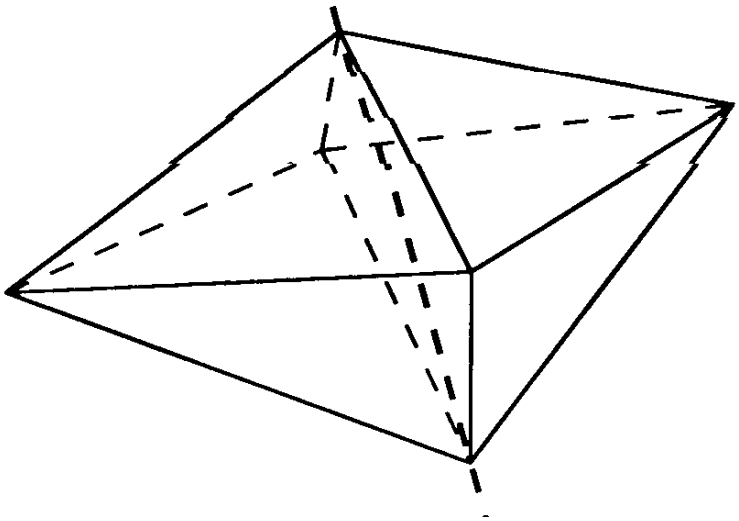

Figure 7: *A four-fold bipyramid. The bond in the center is identified as a +72 degree disclination.*

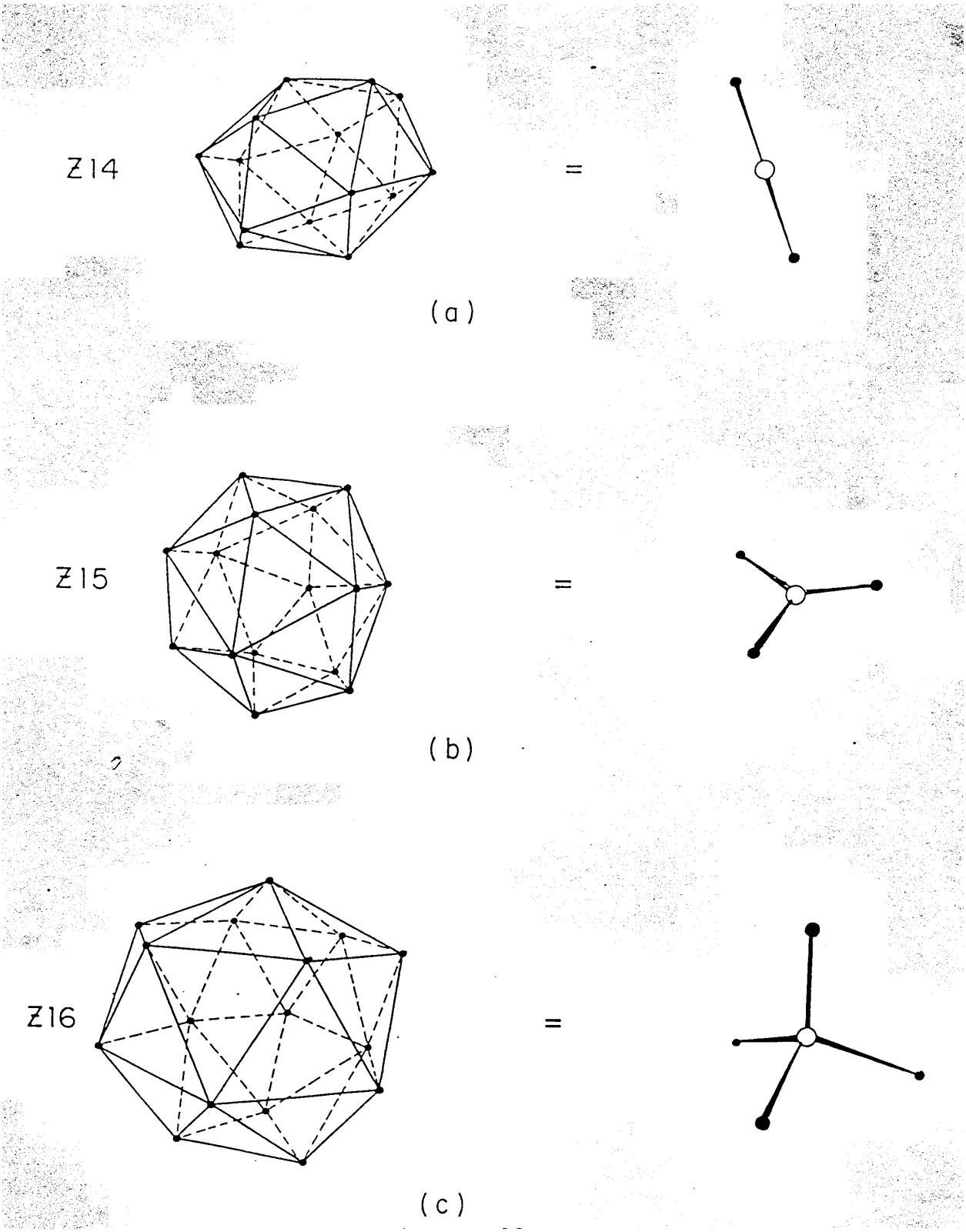

Figure 8: *Fourteen, fifteen and sixteen co-ordinated particles. The figures on the right indicate the six-fold disclination lines emanating from the central atom.*

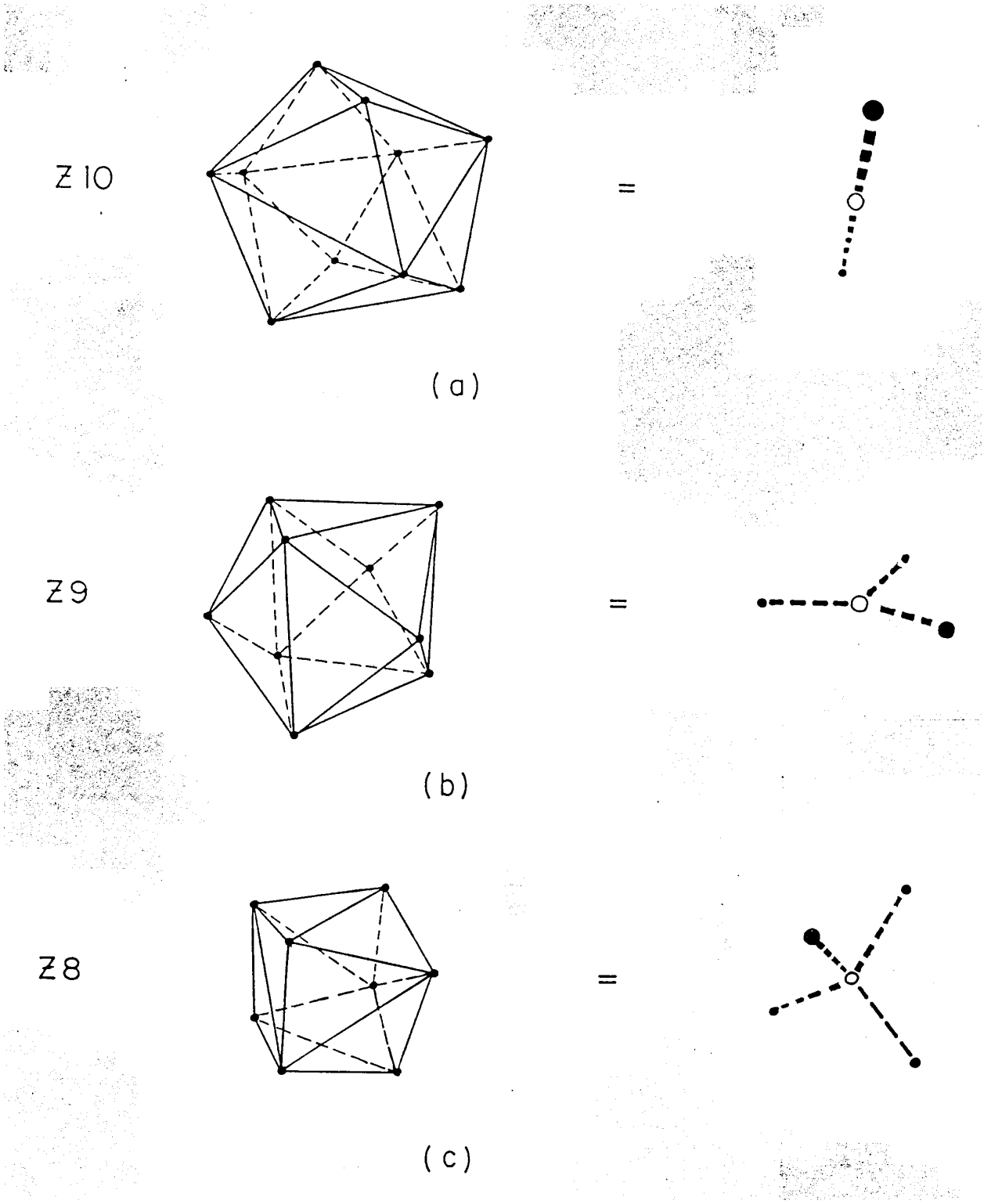

Figure 9: *Eight, nine and ten co-ordinated particles. The figures on the right indicate the four-fold disclination lines emanating from the central atom.*

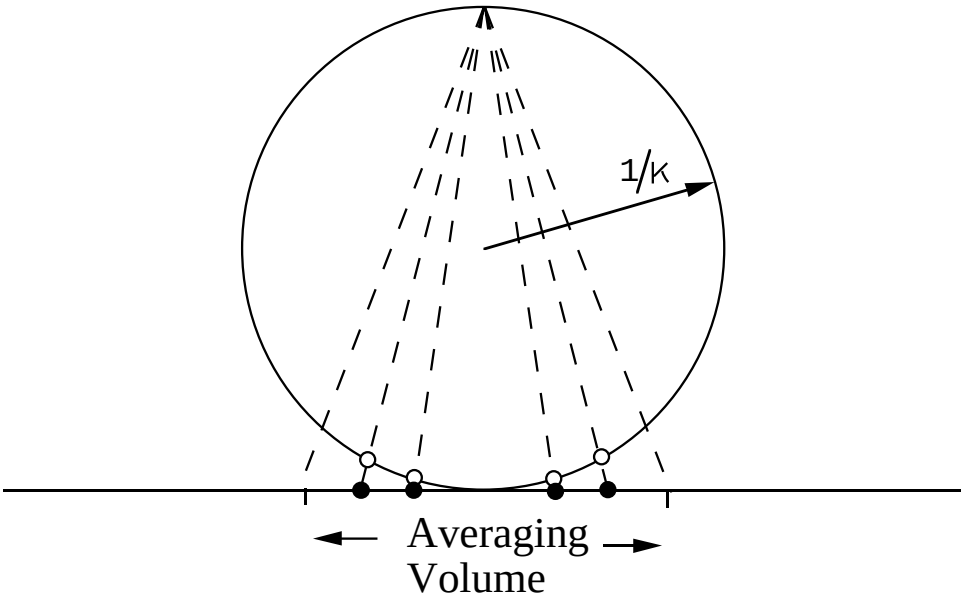

Figure 10: *Schematic showing the projection of a configuration of particles onto a tangent sphere.*

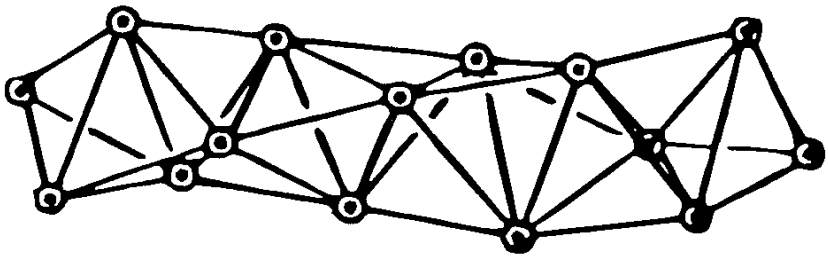

Figure 11: *Tetrahedra forming a Bernal spiral.*

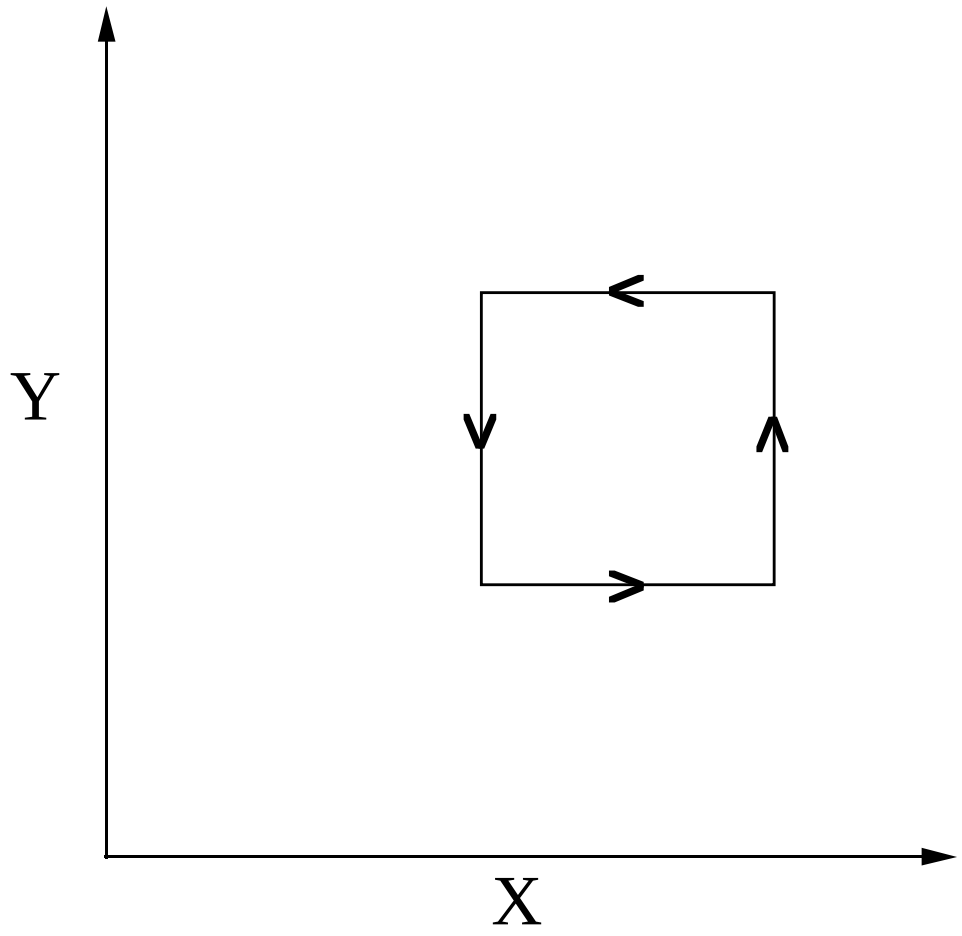

Figure 12: *Rolling the sphere around a closed loop. The final state of the order parameter is related to the initial state by a rotation about an axis perpendicular to the plane of the loop.*

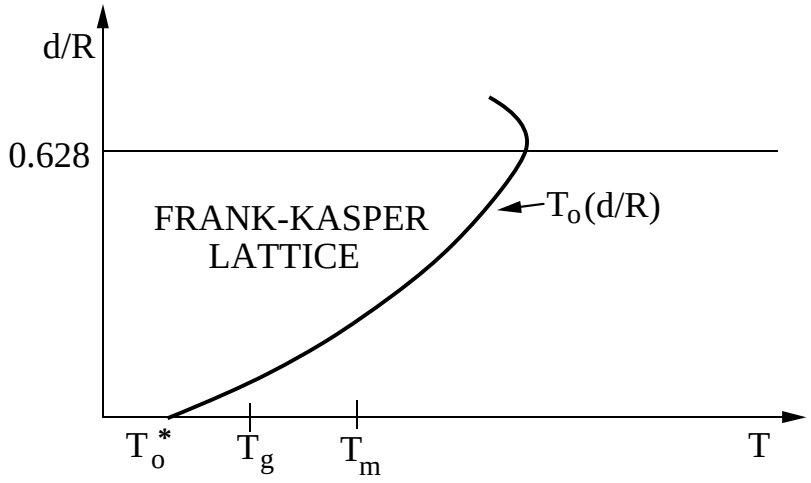

(a)

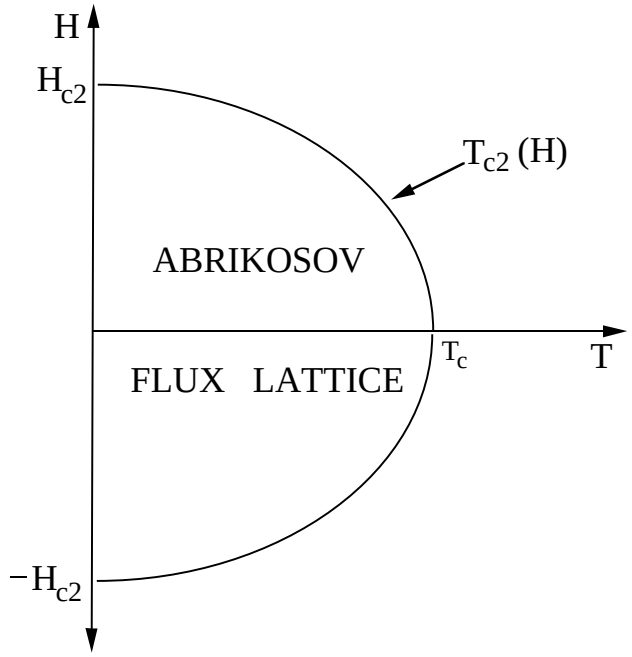

(b)

Figure 13: *(a) Hypothetical phase diagram of simple fluids with short-range icosahedral order as a function of temperature and "curvature"*, i.e. d/R. *$T_0(d/R)$ is the mean field instability temperature of the liquid towards a Frank-Kasper like crystal. Its value in flat space is T_0^*. T_m is the melting temperature of a FCC lattice. Since $N < \infty$, the transitions at finite curvature will, of course be smeared by finite size effects. (b) Phase diagram of an extreme type-II superconductor in a magnetic field. T_c is the critical temperature in the absence of a magnetic field and $T_{c2}(H)$ is the locus of transitions into an Abrikosov flux lattice.*

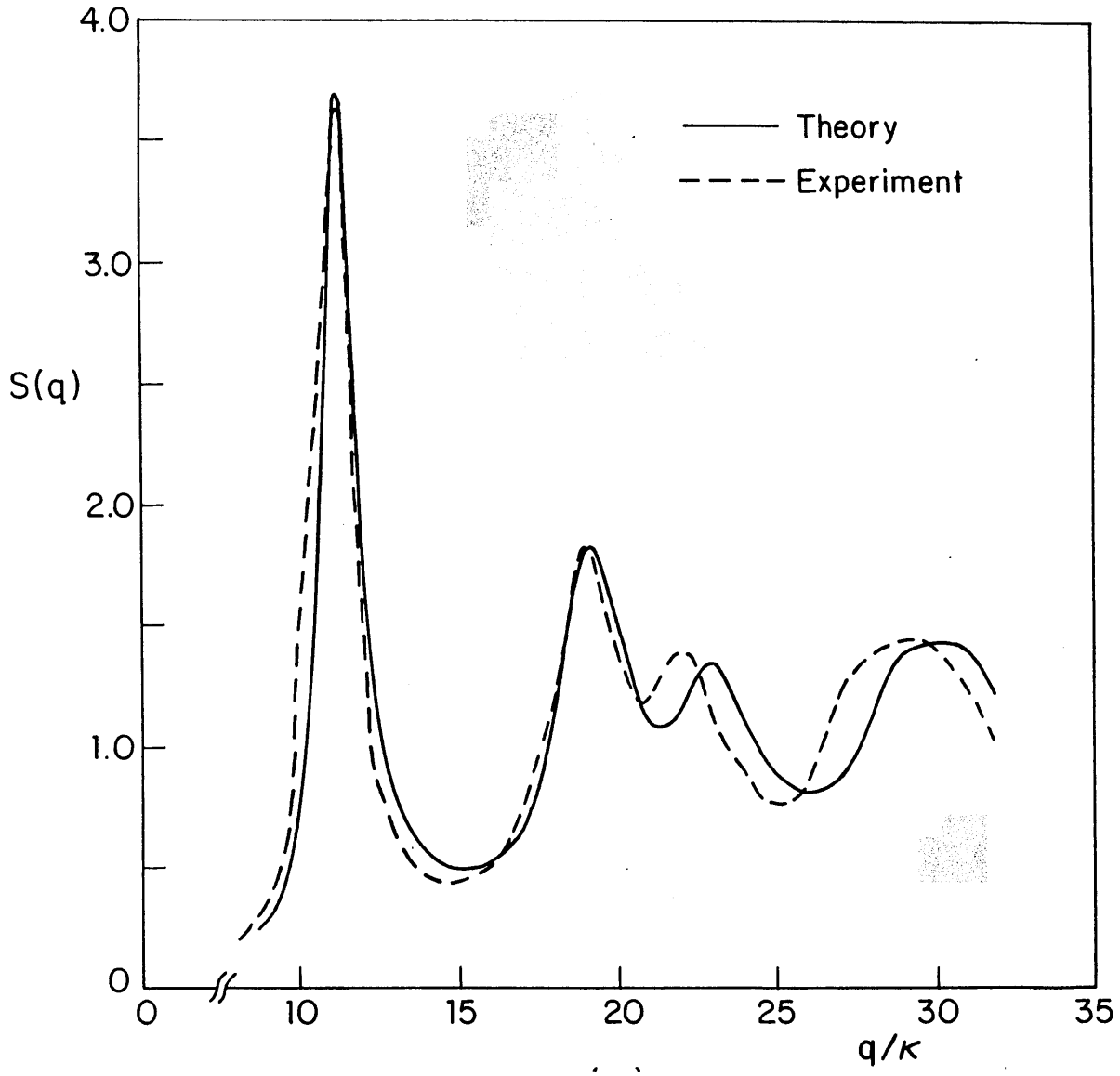

Figure 14: *A comparison of the structure factor obtained by fitting the theoretical prediction to the experimental data on amorphous cobalt films obtained by Leung and Wright. [26] There are two adjustable parameters for each peak which determine its width and height. The peak positions are however a consequence of the theory.*

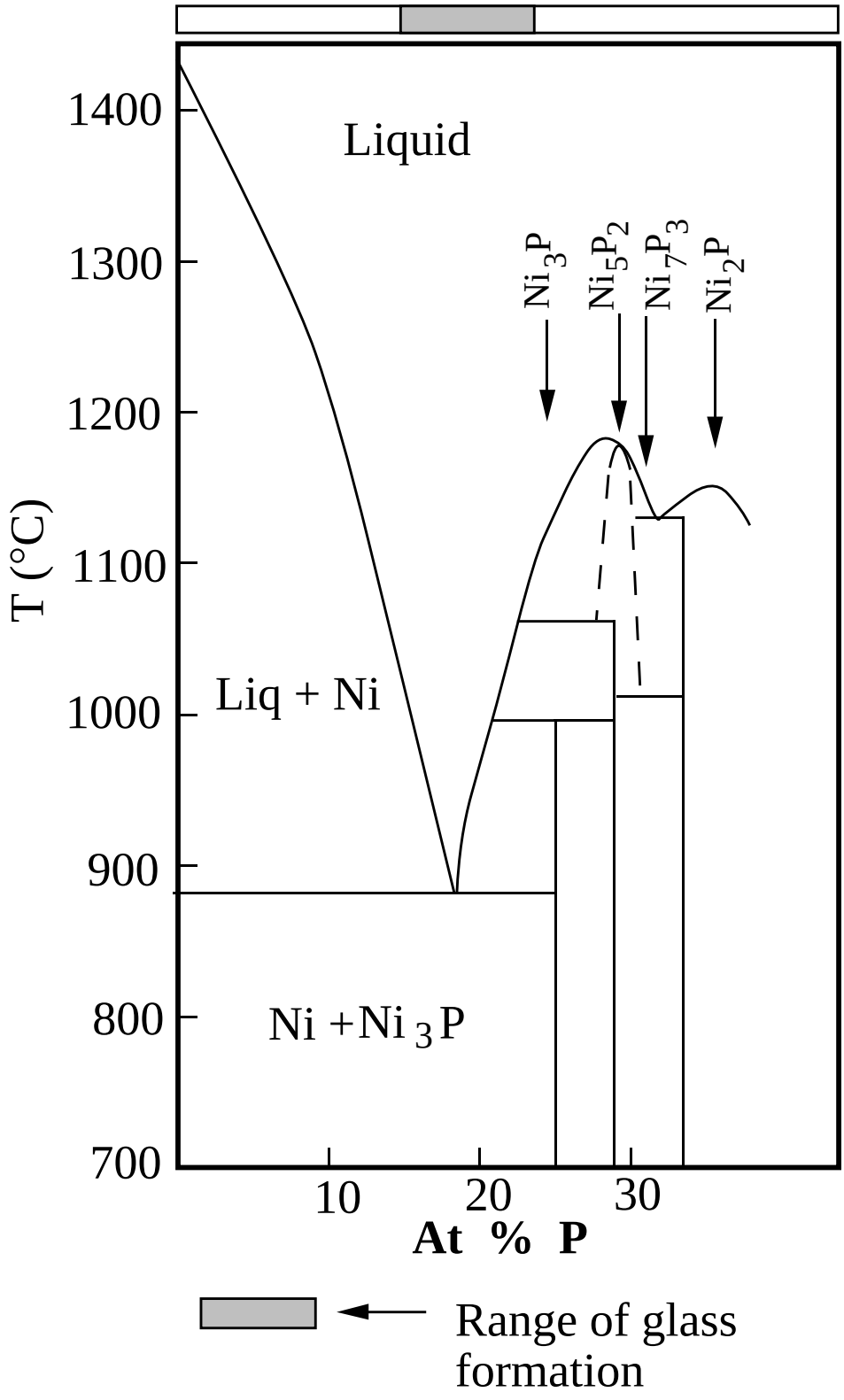

Figure 15: *Phase diagram of the $Ni-P$ system. Also indicated is the range of compositions over which rapid cooling from the melt forms a glass.*

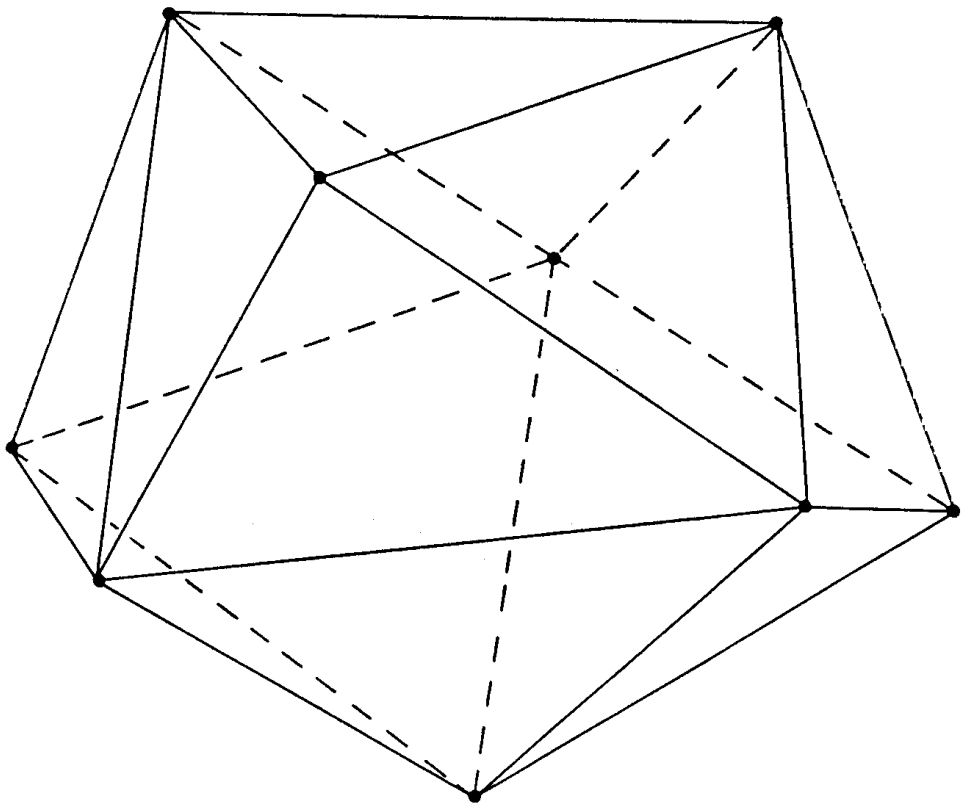

Figure 16: *Co-ordination shell of the P atom in Ni_3P. The topology of this shell is identical to the Z9 defect in Fig 5.9. We denote the number of n-fold bonds emanating from the central P atom by v_n; we have $v_5 = 6$, $v_6 = 0$, and $v_4 = 3$.*

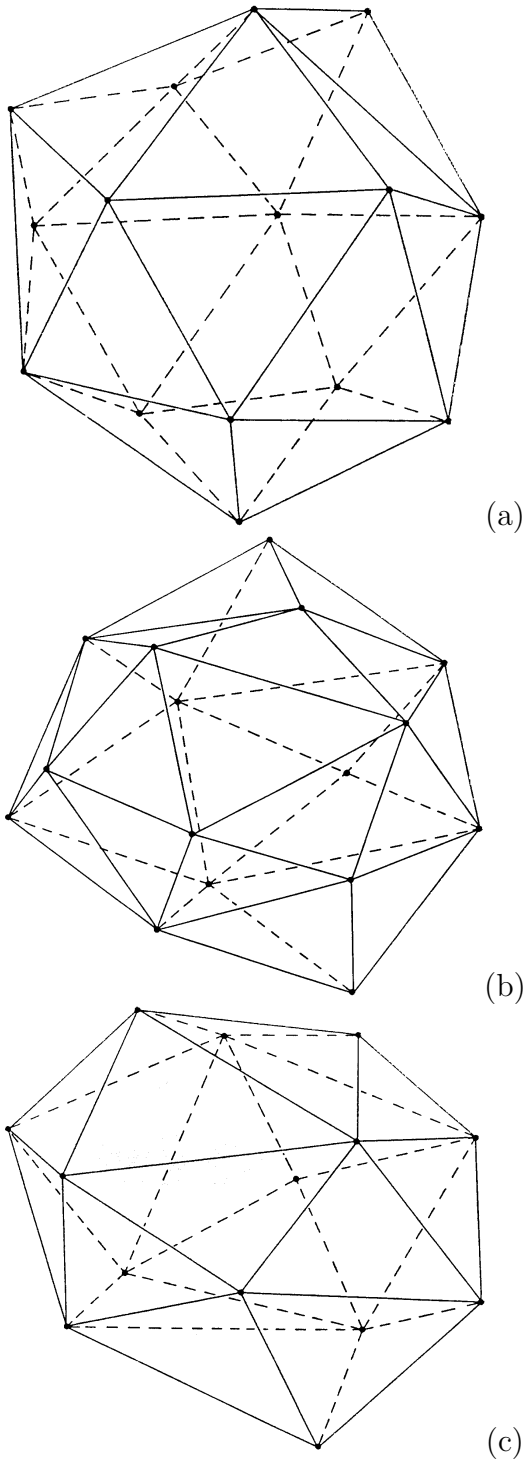

Figure 17: *Co-ordination shell of the* (a) NiI ($v_5 = 10$, $v_6 = 4$, $v_4 = 1$), (b) $NiII$ ($v_5 = 6$, $v_6 = 7$, $v_4 = 3$), (c) $NiIII$ ($v_5 = 6$, $v_6 = 5$, $v_4 = 3$) *atoms in* Ni_3P.